

Evaluation of WRF Mean and Extreme Precipitation over Spain: Present Climate (1970–99)

DANIEL ARGÜESO

Applied Physics Department, Universidad de Granada, Granada, Spain, and Climate Change Research Centre, University of New South Wales, Sydney, New South Wales, Australia

JOSÉ MANUEL HIDALGO-MUÑOZ, SONIA RAQUEL GÁMIZ-FORTIS,
MARÍA JESÚS ESTEBAN-PARRA, AND YOLANDA CASTRO-DÍEZ

Applied Physics Department, Universidad de Granada, Granada, Spain

(Manuscript received 13 May 2011, in final form 13 February 2012)

ABSTRACT

The ability of the Weather Research and Forecasting model (WRF) to simulate precipitation over Spain is evaluated from a climatological point of view. The complex topography and the large rainfall variability make the Iberian Peninsula a particularly interesting region and permit assessment of model performance under very demanding conditions.

Three high-resolution (10 km) simulations over the Iberian Peninsula have been completed spanning a 30-yr period (1970–99) and driven by different datasets: the 40-yr European Centre for Medium-Range Weather Forecasts Re-Analysis (ERA-40) as “perfect boundary conditions” and two general circulation models (GCMs), the Max Planck Institute ECHAM5 model (ECHAM5/MPI) and the NCAR Community Climate System Model, version 3 (CCSM3). The daily precipitation observational grid Spain02 is employed to evaluate the model at varying time scales. Not only are the long-term means (annual, seasonal, and monthly) examined but also the high-order statistics (extreme events).

The WRF provides valuable information on precipitation at high resolution and enhances local spatial distribution due to orographic features. Although substantial errors are still observed in terms of monthly precipitation, especially during the spring, the model is largely able to capture the various precipitation regimes. The major benefits of using WRF are related to the spatial distribution of rainfall and the simulation of extreme events, two facets of climate that can be barely explored with GCMs.

This study shows that WRF can be a useful tool for generating high-resolution climate information for Spanish precipitation at spatial and temporal scales that are crucial for both the environment and human life.

1. Introduction

General circulation models (GCMs) are currently the prime source of information for future climate projections. Indeed, they are extremely useful, providing comprehensive knowledge of the large-scale climate. However, because of their coarse resolution, they are still unable to capture local features of climate and produce detailed information about climate at scales that are crucial to the population and the natural environment.

Dynamical downscaling by means of a regional climate model (RCM) enables the generation of high-resolution projections of climate change scenarios, and thus overcomes the resolution limitation of GCMs. The technique consists of finding an approximate solution to the equations of the atmosphere at high resolution over a confined region, using the GCMs to specify the boundary conditions. As a consequence, RCMs are able to resolve local-scale circulations that the GCMs cannot be expected to capture, providing added-value information with respect to the boundary data (Antic et al. 2006; Laprise 2008). In particular, the benefit of high-resolution simulations is related to those aspects of climate that are essentially local and unevenly distributed, such as precipitation (Rummukainen 2010).

Corresponding author address: Daniel Argüeso, Departamento de Física Aplicada, Facultad de Ciencias, Campus de Fuentenueva s/n, 18071 Granada, Spain.
E-mail: dab@ugr.es

Precipitation plays a critical role in environmental, social, and economic issues (e.g., agriculture, water resources, flood risk), and its accurate description by regional models is crucial to determine possible climate change repercussions. The long-term means must be correctly reproduced because they directly affect water availability and hydrological processes. However, daily precipitation and the associated extreme events must also be captured, since their occurrence and intensity have major effects on the population and the ecosystems. Consequently, it is essential to assess, from a multitemporal viewpoint, the reliability of the high-resolution projections produced by climate models.

The necessity to study both the mean climatic values and the high-order statistics of precipitation has already been emphasized (Leung et al. 2003; Solomon et al. 2007). Several authors (Caldwell et al. 2009; Evans and McCabe 2010; Jacob et al. 2007; Rosenberg et al. 2010) have focused on RCM performance in terms of precipitation and have addressed the extreme event issue to various degrees. They all highlighted that RCMs generally improve rainfall frequency and spatial distribution with respect to the boundary data, although some studies (Boberg et al. 2010; Kjellstrom et al. 2010) obtained unsatisfactory results over southern Europe and especially over the Iberian Peninsula (IP). Although the low observation densities used in these studies may hinder the validation, the poor results are probably a consequence of the Iberian precipitation peculiarities as well.

The IP constitutes an important challenge to RCMs, as evidenced by the studies referenced above. The location in the midlatitudes, which confers large precipitation variability to the area, and the complex topography that characterizes the region makes precipitation especially difficult to simulate. Although it is true that dynamical downscaling is particularly beneficial over regions with complex terrain, the largest deviations from the observations are still located over the mountainous regions (Gao and Giorgi 2008; Heikkilä et al. 2011; Herrera et al. 2010). Precipitation is highly variable over very small distances in these regions and thus significant errors can be obtained due to slight misplacements of rainfall. Many parameterization schemes have been tuned to datasets from pristine surface and environmental conditions (Stensrud 2007) and thus they still have to be validated over complex terrain areas to ascertain their validity. Moreover, the IP is located in the western Mediterranean Sea, a region that is expected to be among those most affected by precipitation decreases across the globe (Christensen et al. 2007). Therefore, the Weather Research and Forecasting model (WRF)'s validation over Spain is not only interesting to produce climate change projections over the region but also might provide valuable information about

regional climate modeling over areas believed to be particularly vulnerable to climate change.

In this study, three 30-yr climate runs were completed at 10-km resolution over the IP with the WRF (Skamarock et al. 2008) to evaluate its capacity to simulate Spanish precipitation and to determine its adequacy for future climate simulations over Spain. The simulations spanned the 1970–99 period and were driven by both observational reanalysis and global models. The use of these two kinds of boundary data made it possible to elucidate whether inadequacies in the simulations were generated by the RCM or inherited from the GCM (Evans and McCabe 2010). Therefore, the suitability of the two different GCM–RCM combinations for climate studies over Spain is explored here in terms of precipitation. Herrera et al. (2010) carried out a similar analysis over Spain using the 25-km RCM simulations included in the ENSEMBLES-based predictions of climate changes and their impacts (ENSEMBLES) project that were driven with 40-yr European Centre for Medium-Range Weather Forecasts Re-Analysis (ERA-40) (Uppala et al. 2005). In the present work, the validation was extended to simulations driven by GCMs and using WRF, which was not included in the aforementioned project. Furthermore, the spatial resolution employed (10 km) has no precedent over 30-yr (climate) intervals, highlighting the state-of-the-art nature of this study of exploring the benefits of applying a finer mesh to the projection of long-term climate.

2. Observational dataset and the regional climate model

a. Observational dataset

The selection of an appropriate dataset to validate the RCMs is certainly not a trivial task. Gridded datasets derived from observations are probably the most adequate tool to validate an RCM because their spatial scales are comparable, in contrast to in situ measurements. Observational gridded datasets, such as the ENSEMBLES daily observational gridded dataset (E-OBS) (Haylock et al. 2008), are usually created using networks that are too sparse over certain areas (e.g., the IP) and thus might be prone to substantial errors, particularly in terms of extreme events. Herrera et al. (2012) have recently developed a daily precipitation grid over Spain using 2756 quality-controlled stations, which amounts to an extraordinarily dense network. The so-called Spain02 dataset is a regular 0.2° (~ 20 km) daily gridded dataset that spans a 54-yr period (1950–2003) and covers peninsular Spain and the Balearic Islands. The density of stations allowed the generation of a high-resolution gridded dataset that accurately captures local

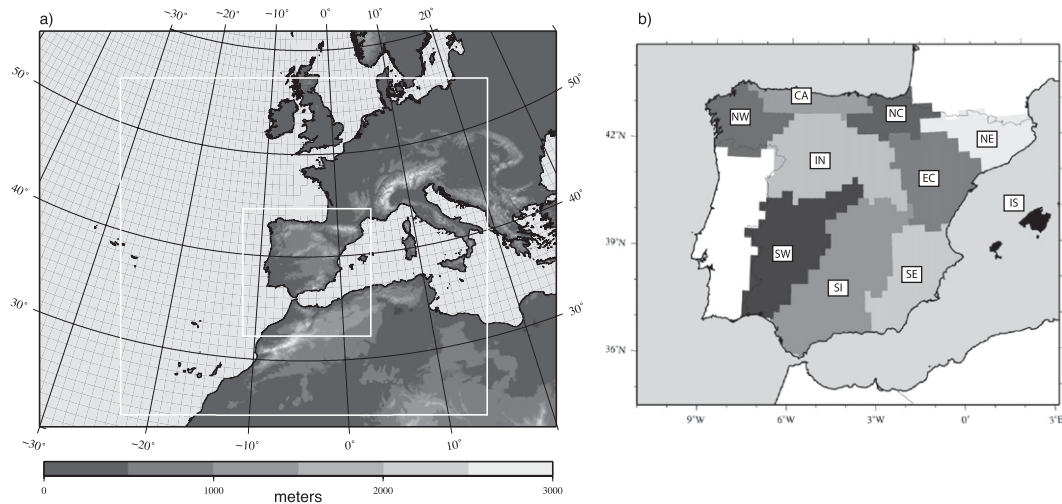


FIG. 1. (a) Topography of the studied region and the location of the WRF domains (white solid lines). (b) The 10 precipitation climate divisions obtained with the multistep technique: northwest (NW), Cantabrian Coast (CA), north central (NC), northeast (NE), islands (IS), east central (EC), interior (IN), southwest (SW), southern interior (SI), southeast (SE).

regimes and the upper percentiles of precipitation (Herrera et al. 2012). The technique used to generate the dataset (ordinary and binary kriging) produces weighted averages of precipitation over the grid cells instead of the local measurements provided by the stations and hence the product is specifically suited for comparison with model estimates.

Precipitation in Spain can be roughly classified within three main regions: the eastern coast, the northern Cantabrian coast, and the south and interior of the IP (Esteban-Parra et al. 1998). During the summer, the latter can be further divided in two regions, northern and southern interior. A broad northwest–southeast decreasing gradient in annual mean precipitation characterizes the region, essentially due to the distance from the storm tracks. Topography also plays a role and contributes to the spatial distribution of precipitation regimes.

The nature of precipitation varies considerably across the region. The eastern coast (EC) rainfall has a marked convective component that produces few but intense events that in general result in low annual precipitation (e.g., $<150 \text{ mm yr}^{-1}$ in the southeast). In contrast, the northwest presents a precipitation regime associated with the presence of Atlantic fronts, characterized by more regular precipitation events and climatological values close to 2000 mm yr^{-1} . There are also some localized centers of high precipitation induced by topography (mountain systems in the interior and south).

In addition, the Spanish rainfall is markedly seasonal due to the seasonal shift of the Azores high pressure center. The Azores high acts as a blocking system during

the summer and drives the fronts toward the IP from October to March.

The spatiotemporal variability in precipitation and the different processes involved in its generation make Spain a region of particular interest in terms of regional climate modeling.

b. The WRF model

The climate simulations over the IP were performed using the Weather Research and Forecasting model version 3.1.1 (Skamarock et al. 2008). The WRF model is a mesoscale numerical weather prediction system that integrates the fully compressible, nonhydrostatic Euler equations in their flux form. It has been developed for both operational forecast and atmospheric research needs, and hence includes a large number of configuration options to meet the requirements of applications at very different spatial and temporal scales.

The spatial configuration of the model consisted of two one-way nested domains. A parent 30-km-resolution domain is formed by 120×130 grid points and covers most of western Europe and a large portion of the northern Atlantic. The finer 10-km resolution composed of 135×135 grid points accommodates the whole IP (Fig. 1). In the vertical, the atmosphere is divided in 35 eta-coordinate levels with its top located at 50 hPa.

The model was driven by ERA-40 to provide “perfect boundary conditions” and two GCMs: 1) the Max Planck Institute ECHAM5 model (Roeckner et al. 2003) and 2) the National Center for Atmospheric Research (NCAR) Community Climate System Model, version 3 (CCSM3) (Collins et al. 2006). These GCMs were selected to force

WRF to examine its suitability for climate change studies over Spain. These three simulations will be referred to from now on as WRFERA, WRFEH5 and WRFCCSM, respectively. In all cases, the boundary conditions were provided every 6 h using a relaxation zone and spectral nudging (von Storch et al. 2000; Waldron et al. 1996). Spectral nudging lessens the effects of the domain design and prevents the model from synoptic-scale climate drifts generated by the formulation of lateral boundary conditions over an open system during long-term simulations (Miguez-Macho et al. 2004). The use of spectral nudging is still controversial, but its application to RCMs makes regional climate modeling a real downscaling procedure rather than a boundary value problem (Rummukainen 2010). In any case, a reasonably weak spectral nudging was used in these simulations, adjusting only waves greater than approximately 3900 km (wavenumber 1) with a 24-h periodicity and only over the coarser domain. No variables were nudged in the planetary boundary layer (PBL), and humidity was not nudged at all.

The physics options were selected in accordance with tests performed in a previous study over a similar region (Argüeso et al. 2011). The WRF single-moment three-class scheme (Hong et al. 2004) was chosen for microphysics because no benefit was gained with more complex and computationally expensive schemes. The cumulus scheme was set to Betts–Miller–Janjić (Betts and Miller 1986; Betts 1986; Janjić 1990, 1994), a deep-layer control, adjustment scheme that includes both deep and shallow profiles. The Asymmetrical Convective Model, version 2 (ACM2) scheme (Pleim 2007) was adopted for the PBL, because it is suited to smoothly change from a combination of local and nonlocal transport under unstable conditions to exclusively local behavior in stable situations. Both longwave and shortwave radiation were parameterized by the NCAR Community Atmosphere Model, version 4 (CAM3). The CAM3 scheme (Collins et al. 2004) is recommended for regional climate because it has an ozone distribution that varies on a monthly basis and allows for updating greenhouse gas concentrations depending on the different Special Report on Emissions Scenarios (SRES), which represents an important advantage for climate change studies. The Noah land surface model (LSM) (Chen and Dudhia 2001) was chosen to represent the land–atmosphere fluxes because of its widespread use in long-term simulations.

The 30-yr simulations were divided into three decadal integrations (1970s, 1980s, 1990s) to optimize computational resources. A conservative 7-month spinup was applied to ensure that all variables, including soil moisture and temperature, reached a dynamical equilibrium between the boundary conditions and the model dynamics.

It also allows the model to be independent from the initial conditions. This is particularly important in the case of GCM-driven simulations, since the boundary data lack the complete set of soil variables to initialize the LSM and hence must be retrieved from an additional data source. Indeed, the soil variables were calculated as a June climatological value from ERA-40 and then used to start the LSM.

3. Evaluation parameters

To compare the WRF estimates with the Spain02 dataset, the WRF grid was projected onto the Spain02 grid using the nearest four points via inverse distance weighting. The selection of the nearest four points stems from the resolution difference between both grids (10 vs 20 km). Therefore, the term *grid point* will hereafter refer to the Spain02 mesh.

A climatological value at each grid point was obtained as the mean annual accumulated precipitation over the 30 yr. The total annual rainfall amounts from Spain02 and WRF were compared using the pattern correlation (Walsh and McGregor 1997), which is essentially a standard Pearson's correlation over the space. As a result, it is possible to determine the model capacity to adequately distribute precipitation across Spain and identify areas where deviations in the annual rainfall are larger.

The seasonal and annual biases for monthly precipitation were calculated to provide further detail of the time-averaged differences between the model and the observational grid.

The ability of the model to describe the annual cycle was also explored by region. To that purpose, the multistep regionalization technique proposed by Argüeso et al. (2011) was conducted to define precipitation climate divisions and then the annual cycle was calculated over the different regions. The technique consists of three concatenated methods [S-mode principal component analysis (PCA), hierarchical clustering, and non-hierarchical clustering] that determine the suitable number and configuration of the affinity areas in an objective way. A 10-division configuration was suggested by the method for Spanish precipitation (Fig. 1b), which appears to be qualitatively consistent with local topography and the distribution of rainfall regimes. However, an in-depth evaluation of the technique is beyond the scope of this paper.

The distribution of precipitation in different intensity events can be studied by the analysis of the probability density function (PDF). Precipitation PDFs are usually skewed toward light rainfall events and extreme events are unlikely. Despite the probability disparity between heavy and light precipitation events, their contribution

to annual rates is equally determinant. Small errors in the simulation of upper-percentile precipitation events might affect total annual rainfall significantly. But large differences in the occurrence of light precipitation also have an effect on annual precipitation deviations. A single plot for the complete spectrum of events might lead to misrepresentation of the PDF deviations because, depending on the scale (linear or logarithmic), the errors on either light or severe precipitation might be given too much importance. In this study, a pseudo-PDF plot is proposed, in which the contribution to total annual precipitation by different intensity events is calculated. As a result, the deviations in precipitation due to different events can be shown in a single plot that covers the entire spectrum. The pseudo-PDFs are calculated for each of the previously identified regions considering all grid points and all wet events ($>0.1 \text{ mm day}^{-1}$) within a region. The model's ability to reproduce the precipitation PDF is further explored with the Perkins skill score (SS; Perkins et al. 2007), which quantifies the common area between the modeled and the observed PDF at each grid point.

Finally, a number of extreme indices selected from those suggested by the Expert Team on Climate Change Detection and Indices (ETCCDI, <http://cccma.seos.uvic.ca/ETCCDI/>) were also calculated. These indices were the maximum 5-day precipitation (Rx5day), the number of days that exceed 10 mm (R10), the percentage of precipitation explained by events within the 95th percentile (R95T), the mean annual number of maximum consecutive dry days (CDD*), and the mean annual number of maximum consecutive wet days (CWD*). Please note that the original CDD and CWD indices were not defined as annual means but as absolute maxima over the studied period. Other indices, such as the maximum 1-day precipitation (Rx1day), the number of days that exceed 20 mm (R20), or the simple daily intensity index (SDII), were also calculated but are not shown because they did not give supplementary information in the assessment of the model performance.

4. Results and discussion

In this section, the precipitation estimates of WRF driven by different boundary conditions are evaluated against the Spain02 observational gridded dataset.

a. Annual, seasonal, and monthly precipitation

Figure 2 illustrates the climatological annual precipitation for the period 1970–99. The pattern correlation shown in brackets is a measure of the ability to correctly

distribute the precipitation over the region; however, it is not sensitive to biases and thus only explains the spatial similarity of the various maps. All three simulations, driven by ERA-40, ECHAM5, and CCSM, show considerably high correlations (0.80–0.83), which indicates that the model is able to recreate the influence of topographical features on precipitation and describe the broad gradient from southeast to northwest. The pattern correlations directly calculated for the boundary data precipitation fields were 0.75 for ERA-40, 0.57 for ECHAM5, and 0.65 for CCSM.

In general, WRF compares well with the observations when driven by perfect boundary conditions (ERA-40), except for some local deviations, mainly in the northwest. In contrast, the GCM-nested simulations produce significant errors in the total annual precipitation in certain regions, although they are highly spatially correlated with observations. To be specific, the WRF5 simulations tend to produce an excess of rainfall in the northwestern quarter, whereas WRFCCSM tends to enhance the southeast–northwest precipitation gradient.

Figure 3 explicitly shows these WRF deviations with respect to the observations at seasonal and annual time scales. The relative biases stress how differently the three simulations behave. WRFERA produces remarkably good results in most of Spain and all through the year, although some positive biases are observed in the northern interior of the Iberian Peninsula, particularly during the spring. In addition, the model also overestimates precipitation, especially during the summer, over certain mountain ranges, such as the Pyrenees in the north and the Sierra Nevada in the south. The WRF model performance is outstanding during the autumn, when the bias remains below 25% over practically the entire region. Autumn rainfall accounts for a large part of the total annual precipitation in many areas over Spain and indeed, the low biases during this season are later reflected in the annual deviations.

The simulations driven by GCMs yield contrasting results in terms of precipitation biases. The major deviations are found during the winter and spring for WRF5, and summer and autumn for WRFCCSM. Unlike the autumn biases that might have a large contribution to the annual total precipitation, summer deviations do not significantly affect annual precipitation because very little rainfall occurs during these months. However, a proper representation of the summer events is also important in terms of describing hydrological stress and droughts, especially along the eastern coast. Additionally, precipitation in the eastern coast is characterized by frequent extreme events during the late summer that should be captured adequately and are caused by warm Mediterranean surface waters that enhance convective

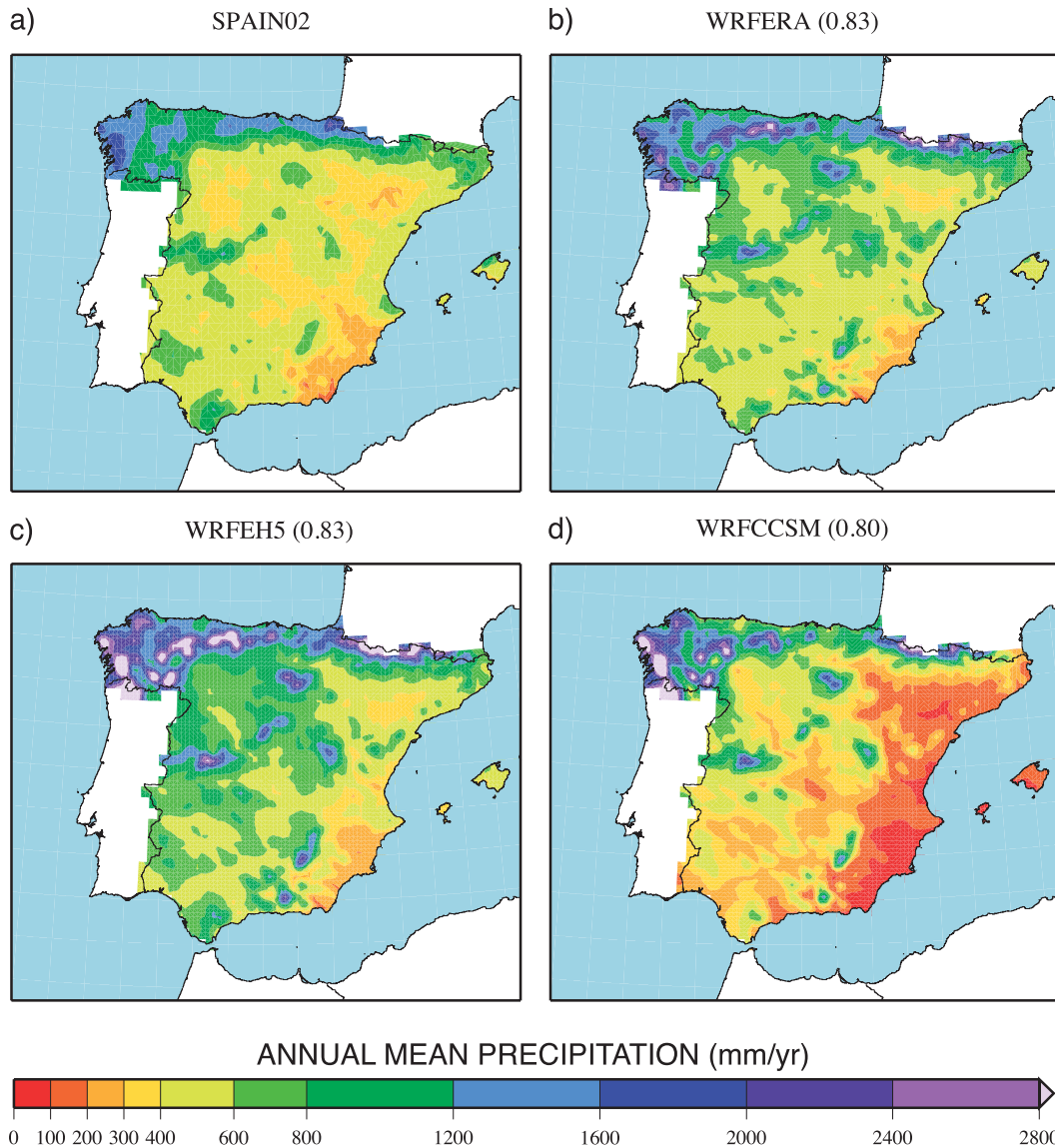


FIG. 2. Climatological annual precipitation (1970–99) for the (a) Spain02 dataset, (b) WRFERA, (c) WRFEH5, and (d) WRFCCSM. The pattern correlation between the WRF simulations and the observational dataset Spain02 are in parentheses.

processes (Romero et al. 1999; Sotillo et al. 2003). This will be examined further in the extreme event analysis.

The GCM-driven simulations tend to produce deviations with opposite sign, but they both present a very similar spatial pattern. The northwest is characterized by positive-to-neutral biases, whereas negative-to-neutral deviations are typical over the eastern coast. The equivalence in the spatial patterns might be interpreted as the regional model ability to distribute precipitation according to topography, regardless of the large-scale biases introduced by the boundary conditions.

Despite the fact that there must be other mechanisms in play (such as a poor simulation of the Mediterranean cyclogenesis processes or misrepresentation of the local topography), the large scale forced by the GCMs shows a similar structure in both cases that induces significant errors. Figure 4 illustrates the seasonal sea level pressure (SLP) mean fields over the coarser domain. Bearing in mind that the SLP in the WRF is largely determined by the boundary conditions, especially when using spectral nudging, we might consider the SLP from WRFERA as quite close to reality. The comparison between seasonal SLP means

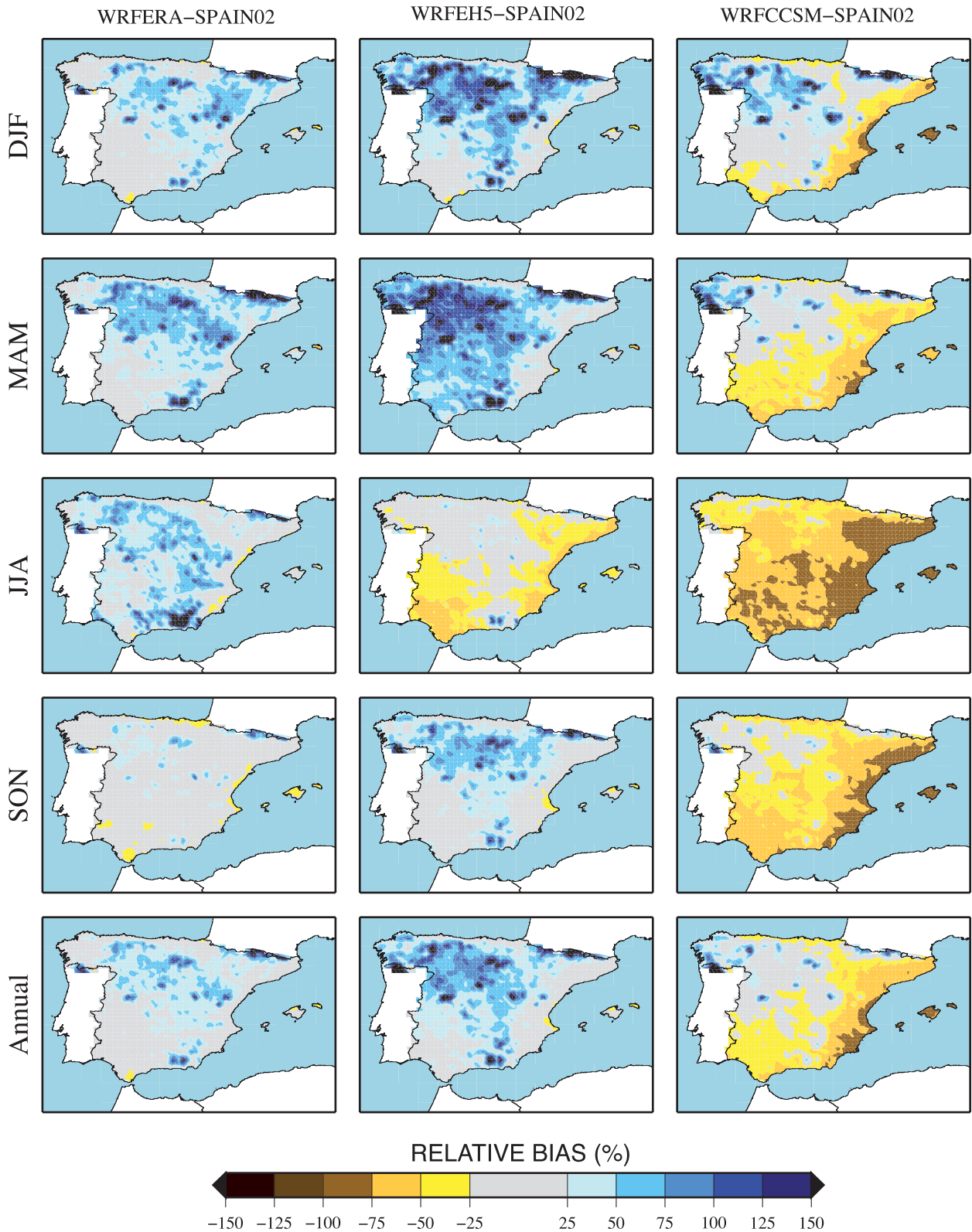


FIG. 3. WRF seasonal and annual precipitation bias compared with Spain02. The biases are written in relative terms (%) with respect to seasonal and annual climatological means (1970–99). (left to right) WRFERA, WRFEH5, and WRFCCSM. (top to bottom) The seasonal [December–February (DJF), March–May (MAM), June–July (JJA), and September–October (SON)] and the annual biases.

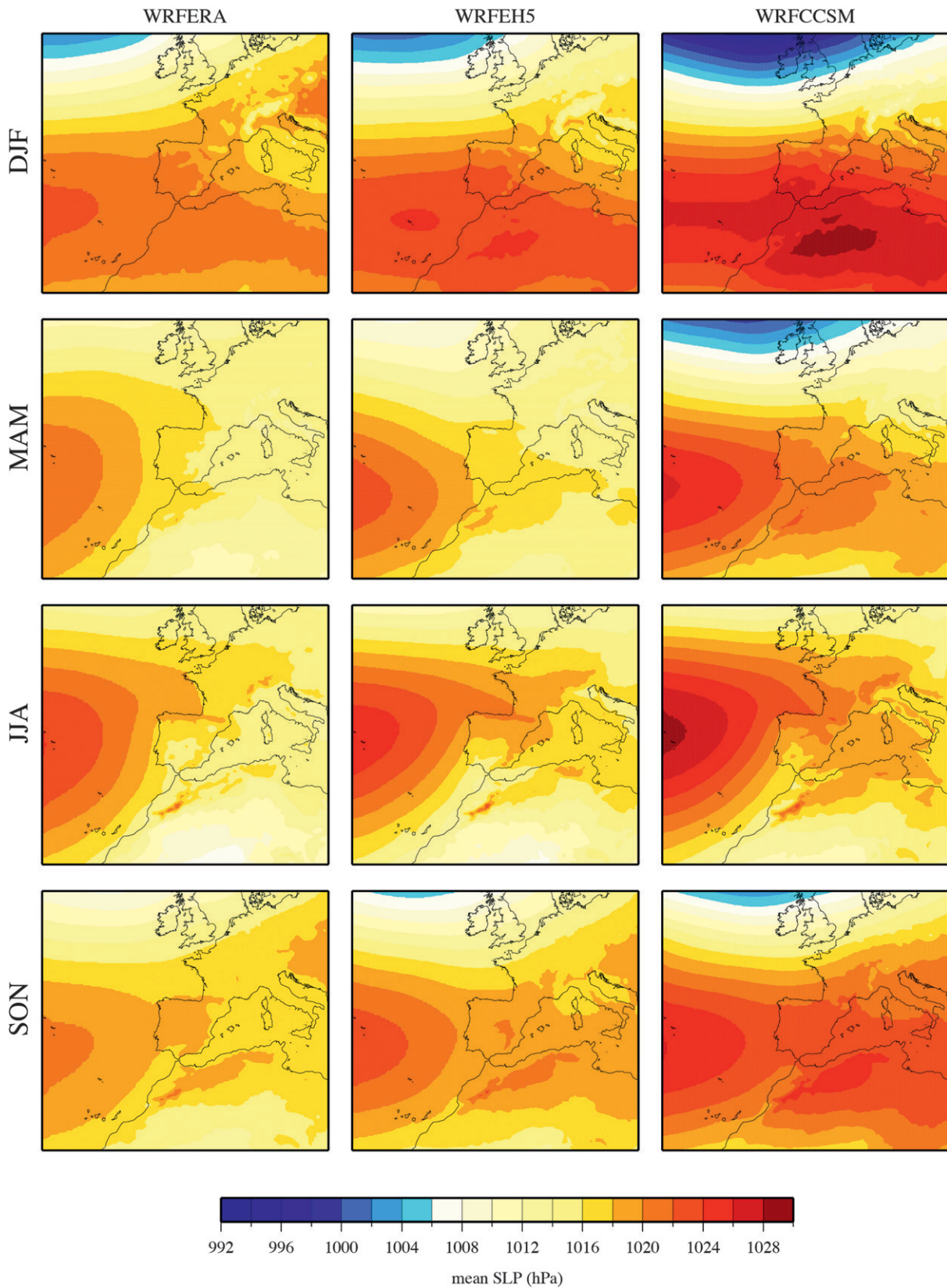


FIG. 4. Seasonal mean SLP fields for WRF simulations over the coarser domain.

from WRFERA and the GCM-driven simulations explains, at least partially, the seasonal precipitation biases. The GCMs force WRF toward a too-zonal circulation and strengthen the north–south pressure gradient (winter, spring, and autumn), which is particularly manifest in the WRFCCSM run. As a consequence, the storm tracks are channeled toward the north, producing a precipitation deficit in the south and east of the IP. In contrast, WRF simulates larger amounts of precipitation in the northern areas because more systems tend to reach this region. During the summer, WRF tends to generate too little precipitation over nearly all of Spain because both GCMs enhance the Azores's blocking system.

The marked seasonality is an important feature of precipitation in the midlatitudes, and is so in the IP. The Spanish annual cycle is characterized by a clearly identifiable dry season, with a monthly minimum that systematically occurs in August, and wet seasons that occur in different periods of the year, even for proximate regions. The annual cycle is here explored over the 10 precipitation regions shown in Fig. 1b.

In general, the shape of the annual cycle is well reproduced by the model (Fig. 5), although it is worth mentioning that WRF also produces substantial errors. While WRFCCSM tends to smooth the annual cycle, removing most of the peaks, WRFERH5 is prone to exaggerate the seasonality. All simulations reproduce the minimum in precipitation during the summer months, but WRFCCSM systematically underestimates it. Precipitation from December to April is broadly overestimated by all simulations, although WRFCCSM shows both under and overestimations depending on the region. There are areas where these deviations are particularly significant, such as the interior region (IN) and the northeastern region (NE). Conversely, monthly rainfall is fairly accurate from May to September in almost all the regions. It is also noticeable that WRFERH5 produces the spring precipitation maximum in advance, bringing it forward 1 month. Thus, although the maximum rainfall generally occurs in May (April) in Spain, WRFERH5 usually predicts a peak in April (March).

The simulation nested in ERA-40 provides excellent results. The shape of the annual cycle is reproduced in most of its details over nearly all of Spain. The rainfall from January to May is overall overestimated; however, from June to December the WRF performance is strikingly accurate, and the WRFERA annual cycle almost overlaps with that of Spain02 in many regions. This is a good indicator of WRF's ability to generate precipitation correctly when nested in good-quality boundary conditions, because it is precisely during the

summer and early autumn that precipitation is mainly controlled by local factors and thus the model parameterizations have a larger impact on rainfall outputs.

b. Daily precipitation events

The accurate description of the precipitation PDF, the probability of a particular event to occur, is crucial for characterizing precipitation regimes. To compute the PDF, only the rainy days (>0.1 mm) were considered because the probability of rainfall intensity is to be examined rather than the precipitation occurrence.

To analyze how WRF reproduces the shape of the PDF, the pseudo-PDF plot is used here as an alternative to standard PDF plots. Figure 6 illustrates the amount of annual precipitation grouped by events. Each value represents how much precipitation is caused by events of particular intensity. A common deficiency of climate models is that they tend to produce too much light precipitation and underestimate the severe events (Bukovsky and Karoly 2011; DeMott et al. 2007; Gutowski et al. 2003). The first part of the statement is confirmed here, but the second one is not clearly evidenced in our simulations.

The overall shape of the pseudo-PDF is well captured by WRF, except in the eastern regions [southeast (SE), east central (EC), and islands (IS)], where WRF misplaces the maxima. All simulations assign the maximum contribution to events between 1 and 5 mm day⁻¹, whereas the observations locate the maximum between 5 and 10 mm day⁻¹. The WRF model generally produces too many rainfall events from 0.1 to 15 mm day⁻¹, except for WRFCCSM, which only overestimates the contribution from events below 5 mm day⁻¹. Actually, errors in the occurrence of events within the bins 1–5 and 5–10 mm day⁻¹ amount to an important bias contribution, over 100 mm yr⁻¹ in regions such as the interior (IN) or north central (NC). Along the eastern coast (SE, EC, or IS), these errors might be especially significant in relative terms because the annual rainfall rates are smaller.

The frequency of events that exceed 20 mm day⁻¹ are accurately described by WRFERA in the majority of the regions with minor underestimations, except in the northeast (NE) (overestimated) and in the IS (markedly underestimated). The other two simulations present contrasting performances. WRFCCSM tends to underestimate extreme events [apart from the northwest (NW), where all WRF runs present a clearly distinct behavior], whereas WRFERH5 returns satisfactory results with moderate overestimation. As for the very extreme events accommodated in the last bin (>80 mm day⁻¹), two features are remarkable: 1) a clear underestimation in the SE and IS regions

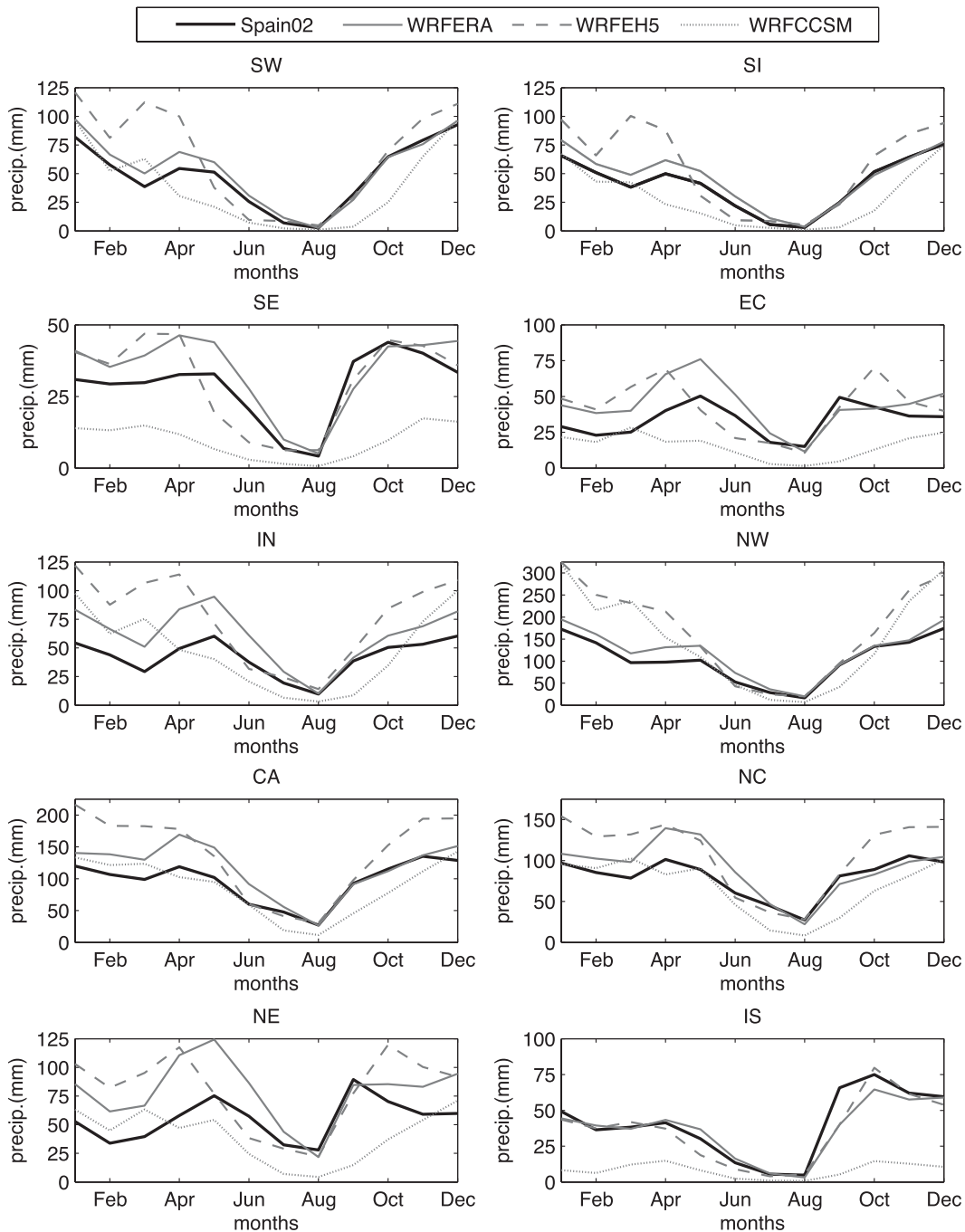


FIG. 5. Precipitation annual cycle in the different regions.

and 2) a substantial overestimation in the northern regions, particularly in the NW and the NE.

These characteristics of simulated precipitation regimes are in accordance with previous results. Indeed, areas where both WRFERA and WRFEH5 led to positive seasonal biases show a systematic overestimation of almost all types of events. Conversely,

the complete range of events is underestimated by WRFCCSM over the Mediterranean regions (SE, EC, NE, and IS).

This analysis supports the idea that the problem of the precipitation PDF simulation might not be directly attributed to the WRF's deficiencies, but rather to boundary conditions (except for the light precipitation

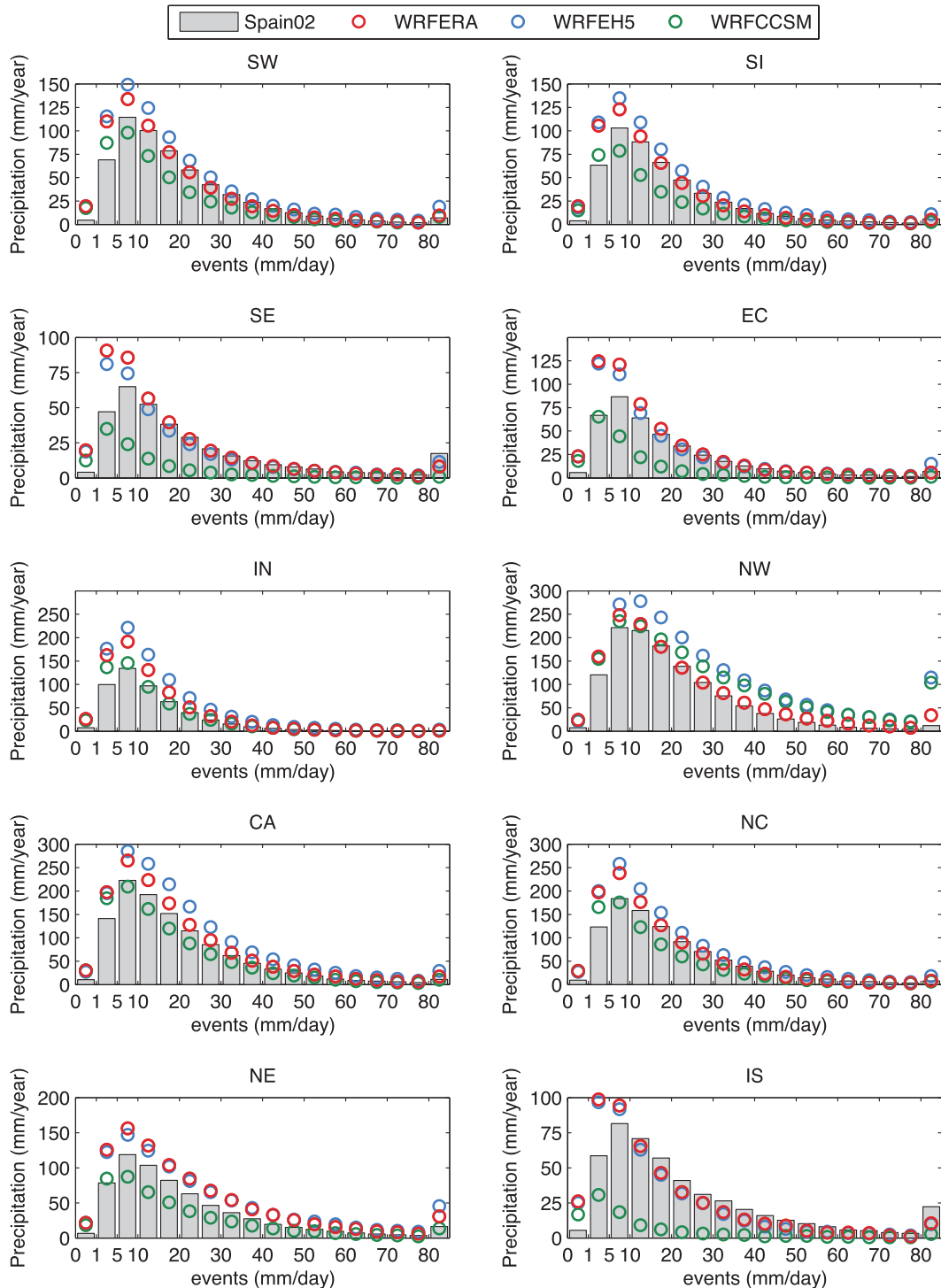


FIG. 6. Contribution to total annual precipitation from different intensity events in the 10 precipitation regions.

overestimations). In most of the regions, the WRF simulation that was nested in perfect boundary conditions provided fairly good results in terms of the precipitation event intensity.

In addition to the pseudo-PDF, a spatial analysis of the similarity between two PDFs is conducted using the SS (Fig. 7). In this case, the SS is computed from a PDF calculated using 1-mm bins and ranging from

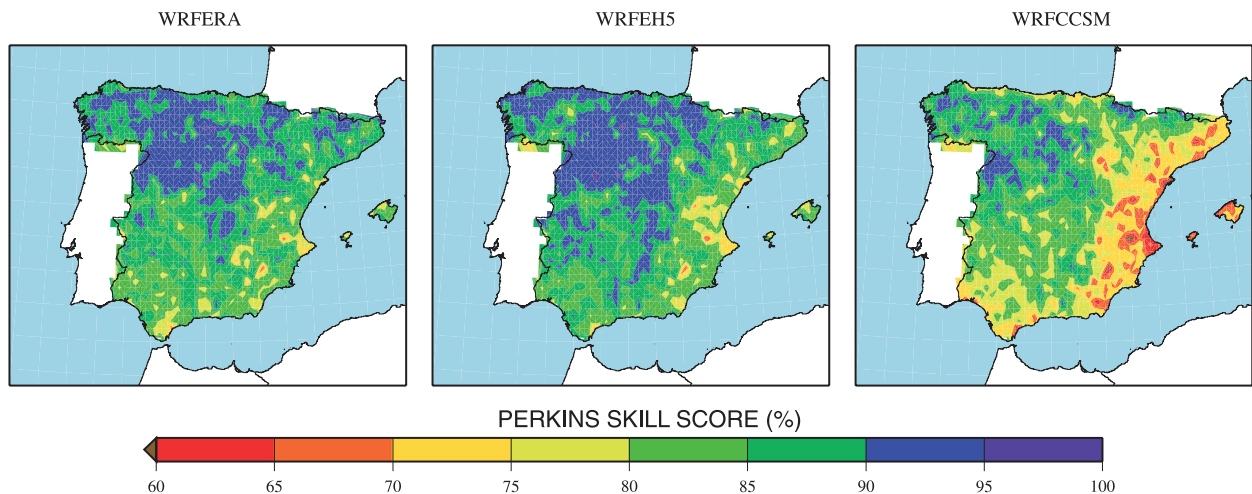


FIG. 7. Spatial distribution of the SS (%) with respect to Spain02 for (left to right) WRFERA, WRFEH5, and WRFCCSM simulations.

0 to 120 mm day^{-1} . The SS reaches its lowest values in the eastern part of Spain, a region that is characterized by frequent confined downpours that have their origin in the Mediterranean and are forced by local topography. These values are particularly low for WRFCCSM (down to 52%). For the other two simulations, the SS remains between 80% and 100% in nearly all grid points. All simulations reach the largest SS values in the northwest and the northern interior, where precipitation is more regular and generated by large-scale fronts, and thus easier to simulate by RCMs.

c. Extreme indices

Two different classes of indices are examined here: 1) a group that illustrates the high-order statistics (Rx5day, R10, and R95T) and 2) a group that represents the persistence of both wet and dry periods (CWD* and CDD*). Figure 8 shows the values of these extreme indices calculated for Spain02 and the WRF simulations.

The indices that concern the heavy rainfall are in general well represented by WRFERA in both magnitude and spatial distribution. In turn, the GCM-driven simulations also capture their spatial distribution adequately but fail to predict their magnitude.

The Rx5day presents lower values in the interior plateau but higher ones in mountainous areas, in the northwest, and especially along the eastern coast. WRFERA generates a very similar pattern but tends to lessen the index over the central eastern coast and the southern mountains by more than 100 mm. In contrast, it intensifies the Rx5day in the internal mountains and strengthens the high values over the northwest. WRFEH5 tends to enhance the maxima located over the mountain systems throughout the region, whereas

WRFCCSM underestimates this index in most of Spain, except for the mountains in the interior and the northwest.

As for the R10 index, the broad gradient from the southeast to the northwest is accurately represented by all simulations, although WRFERA produces some local overestimations in the northwestern mountains and the GCM-driven simulations overestimate R10 in the north. In addition, WRFCCSM tends to generate lower R10 than the observations over a wide area in the east, which is probably caused by the general underprediction of precipitation, as found in the analysis of the seasonal biases. On the contrary, WRFEH5 compares well with the observed R10 index in most of the Spanish regions, with errors that seldom exceed 10 days yr^{-1} .

In accordance with the description of precipitation regimes over Spain, it can be observed that the R95T index reaches a maximum over the eastern coast, where very extreme events explain as much as 30% of total annual precipitation. All three simulations adequately reproduce this feature of climate, but all of them tend to intensify the magnitude of this index in nearly the entire region. However, except for the east and some mountain ridges, where the overestimation is appreciable, the three simulations yield values that fall within an error of 2% with respect to Spain02.

Regarding the indices that refer to persistence (CWD* and CDD*), WRF's performance depends strongly on the boundary conditions. The most remarkable differences between WRF and Spain02 are found for the CCSM-driven simulations in terms of the CDD*. WRFCCSM produces more than double the number of CDD* in some locations, such as the eastern coast. Nevertheless, the differences in the CWD* are not as dramatic and WRFCCSM is able to

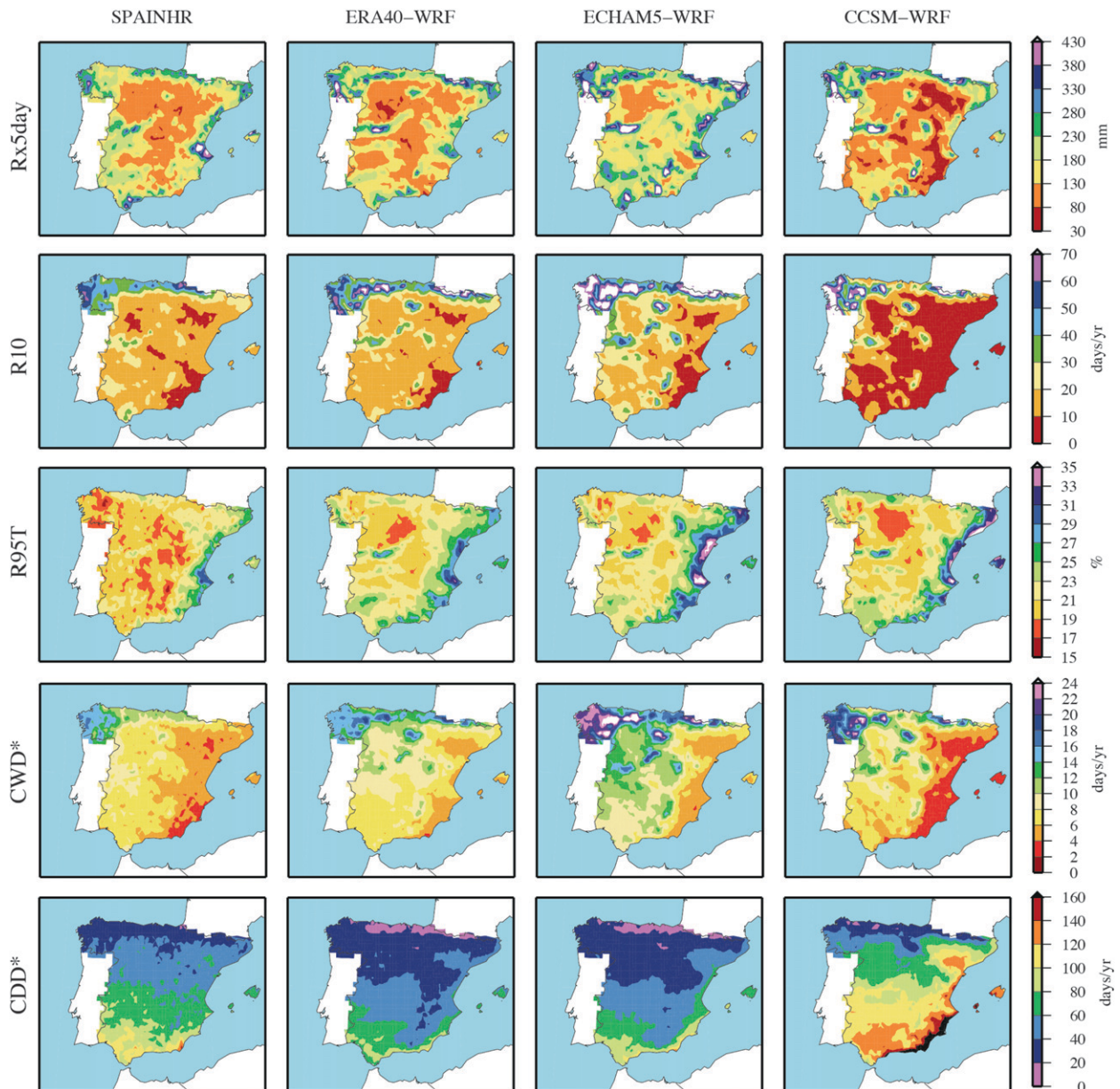


FIG. 8. Extreme indices proposed by ETCCDI for (left to right) Spain02, WRFERA, WRFEH5, and WRFCCSM. The different extremes are displayed by (top to bottom) Rx5day, R10, R95T, CWD*, and CDD*. White areas indicate off-the-scale values.

recreate the values obtained from Spain02, except for slight overestimations in the northwest and underestimations in the east. WRFEH5 yields similar results to WRFCCSM for CWD*, although the overestimation in the northwest is more pronounced. However, it provides much better estimates of CDD* since the errors barely exceed 30 days in a region where CDD* usually reaches 100 days. The WRFERA simulation produces satisfactory results concerning the persistence, despite slight deviations for both CDD* and CWD*. The intricate spatial patterns that these indices present are somehow smoothed by

WRF, but the broad pattern generated by the model compares well with Spain02.

5. Conclusions

All the WRF simulations provide detailed and valuable information on precipitation regimes over a region that is particularly challenging due to its topography and variability, including those forced by GCMs. Despite the uncertainties associated with these GCM-driven simulations, which are not yet negligible and

hence should not be disregarded, it has been proven that the WRF constitutes a beneficial contribution to present and future climate studies over Spain, particularly for exploring facets of climate for which GCMs are inadequate.

Indeed, the main advantage of using the WRF is the possibility to study the climate at scales for which GCMs were not designed. The model is able to correctly distribute precipitation all over Spain, which indicates that it is efficient at differentiating the climate regimes within the region and incorporating the effect of small topographical features. Both WRFERA and WRFEH5, and to a lesser extent, WRFCCSM, show a good skill with respect to the spatial distribution of extreme indices. This is also a sign of the model's ability to reproduce events that usually occur at very small spatiotemporal scales. However, WRF still presents some deficiencies in the magnitudes of these indices, particularly for those characterizing persistence.

Precipitation is fairly well captured at all time scales, although the WRF introduces some substantial seasonal biases over particular regions, principally during the spring. These deviations are highly dependent on deficiencies in the large-scale structures induced by the boundary conditions, as revealed by the SLP analysis. Nonetheless, the regional model must also play a determining role since the spatial patterns of the biases are very similar between the GCM-driven runs. The simulation nested in CCSM tends to reduce seasonal variability and thus produces a flatter annual cycle, whereas WRFEH5 enhances seasonal variability and produces in general an excess of rainfall.

The WRF tends to generate too much light precipitation and to overestimate rainfall in the early months of the year over almost all of Spain, which are not WRF-exclusive features and have been observed in other RCMs. The latter cannot be univocally attributed to a single factor and might be a result of different contributions (e.g., deficiencies in the cloud microphysics treatment, enhancement of the land–sea thermal contrast, deficient simulation of the Mediterranean cyclogenesis). In contrast, during the second half of the year, WRFERA provides outstanding results in most of the regions, which may be regarded as a confirmation of the model's ability to reproduce precipitation when local processes become more decisive (summer and early autumn), provided that accurate boundary conditions are used.

Acknowledgments. The Spanish Ministry of Science and Innovation with additional support from European community funds (FEDER), Project CGL2010-21188/CLI, and the regional government of Andalusia, Project

P06-RNM-01622, have financed this study. The “Centro de Servicios de Informática y Redes de Comunicaciones” (CSIRC), Universidad de Granada, has provided the computing time. Thanks to Dr. Andrew S. Kowalski for his comments and suggestions, which enhanced the clarity of this work. We also thank three anonymous reviewers for their valuable comments, which improved the quality of the manuscript.

REFERENCES

- Antic, S., R. Laprise, B. Denis, and R. de Elia, 2006: Testing the downscaling ability of a one-way nested regional climate model in regions of complex topography. *Climate Dyn.*, **26**, 305–325.
- Argüeso, D., J. M. Hidalgo-Muñoz, S. R. Gámiz-Fortis, M. J. Esteban-Parra, J. Dudhia, and Y. Castro-Díez, 2011: Evaluation of WRF parameterizations for climate studies over southern Spain using a multistep regionalization. *J. Climate*, **24**, 5633–5651.
- Betts, A., 1986: A new convective adjustment scheme. Part I: Observational and theoretical basis. *Quart. J. Roy. Meteor. Soc.*, **112**, 677–691.
- , and M. Miller, 1986: A new convective adjustment scheme. Part II: Single column tests using GATE wave, BOMEX, ATEX and Arctic air-mass data sets. *Quart. J. Roy. Meteor. Soc.*, **112**, 693–709.
- Boberg, F., P. Berg, P. Thejll, W. J. Gutowski, and J. H. Christensen, 2010: Improved confidence in climate change projections of precipitation further evaluated using daily statistics from ENSEMBLES models. *Climate Dyn.*, **35**, 1509–1520.
- Bukovsky, M. S., and D. J. Karoly, 2011: A regional modeling study of climate change impacts on warm-season precipitation in the central United States. *J. Climate*, **24**, 1985–2002.
- Caldwell, P., H.-N. S. Chin, D. C. Bader, and G. Bala, 2009: Evaluation of a WRF dynamical downscaling simulation over California. *Climatic Change*, **95**, 499–521.
- Chen, F., and J. Dudhia, 2001: Coupling an advanced land surface–hydrology model with the Penn State–NCAR MM5 modeling system. Part I: Model implementation and sensitivity. *Mon. Wea. Rev.*, **129**, 569–585.
- Christensen, J. H., and Coauthors, 2007: Regional climate projections. *Climate Change 2007: The Physical Science Basis*, S. Solomon et al., Eds., Cambridge University Press, 847–940.
- Collins, W. D., and Coauthors, 2004: Description of the NCAR Community Atmosphere Model (CAM 3.0). NCAR Tech. Note NCAR/TN-464+STR, 226 pp.
- , and Coauthors, 2006: The Community Climate System Model version 3 (CCSM3). *J. Climate*, **19**, 2122–2143.
- DeMott, C. A., D. A. Randall, and M. Khairoutdinov, 2007: Convective precipitation variability as a tool for general circulation model analysis. *J. Climate*, **20**, 91–112.
- Esteban-Parra, M. J., F. S. Rodrigo, and Y. Castro-Díez, 1998: Spatial and temporal patterns of precipitation in Spain for the period 1880–1992. *Int. J. Climatol.*, **18**, 1557–1574.
- Evans, J., and M. F. McCabe, 2010: Regional climate simulation over Australia's Murray-Darling basin: A multitemporal assessment. *J. Geophys. Res.*, **115**, D14114, doi:10.1029/2010JD013816.
- Gao, X., and F. Giorgi, 2008: Increased aridity in the Mediterranean region under greenhouse gas forcing estimated from high resolution simulations with a regional climate model. *Global Planet. Change*, **62**, 195–209.

- Gutowski, W., Jr., S. Decker, R. Donavan, Z. Pan, R. Arritt, and E. Takle, 2003: Temporal-spatial scales of observed and simulated precipitation in central U.S. climate. *J. Climate*, **16**, 3841–3847.
- Haylock, M. R., N. Hofstra, A. M. G. Klein Tank, E. J. Klok, P. D. Jones, and M. New, 2008: A European daily high-resolution gridded data set of surface temperature and precipitation for 1950–2006. *J. Geophys. Res.*, **113**, D20119, doi:10.1029/2008JD010201.
- Heikkilä, U., A. Sandvik, and A. Sorteberg, 2011: Dynamical downscaling of ERA-40 in complex terrain using the WRF regional climate model. *Climate Dyn.*, **37**, 1551–1564, doi:10.1007/s00382-010-0928-6.
- Herrera, S., L. Fita, J. Fernández, and J. M. Gutiérrez, 2010: Evaluation of the mean and extreme precipitation regimes from the ENSEMBLES regional climate multimodel simulations over Spain. *J. Geophys. Res.*, **115**, D21117, doi:10.1029/2010JD013936.
- , J. M. Gutiérrez, R. Ancell, M. R. Pons, M. D. Frías, and J. Fernández, 2012: Development and analysis of a 50-year high-resolution daily gridded precipitation dataset over Spain (Spain02). *Int. J. Climatol.*, **32**, 74–85, doi:10.1002/joc.2256.
- Hong, S.-Y., J. Dudhia, and S. Chen, 2004: A revised approach to ice microphysical processes for the bulk parameterization of clouds and precipitation. *Mon. Wea. Rev.*, **132**, 103–120.
- Jacob, D., and Coauthors, 2007: An inter-comparison of regional climate models for Europe: Model performance in present-day climate. *Climatic Change*, **81** (Suppl.), 31–52.
- Janjić, Z. I., 1990: The step-mountain coordinate: Physical package. *Mon. Wea. Rev.*, **118**, 1429–1443.
- , 1994: The step-mountain eta coordinate model: Further developments of the convection, viscous sublayer, and turbulence closure schemes. *Mon. Wea. Rev.*, **122**, 927–945.
- Kjellstrom, E., F. Boberg, M. Castro, J. Christensen, G. Nikulin, and E. Sanchez, 2010: Daily and monthly temperature and precipitation statistics as performance indicators for regional climate models. *Climate Res.*, **44**, 135–150.
- Laprise, R., 2008: Regional climate modelling. *J. Comput. Phys.*, **227**, 3641–3666.
- Leung, L. R., L. Mearns, F. Giorgi, and P. H. Wilby, 2003: Regional climate research: Needs and opportunities. *Bull. Amer. Meteor. Soc.*, **84**, 89–95.
- Miguez-Macho, G., G. Stenchikov, and A. Robock, 2004: Spectral nudging to eliminate the effects of domain position and geometry in regional climate model simulations. *J. Geophys. Res.*, **109**, D13104, doi:10.1029/2003JD004495.
- Perkins, S. E., A. J. Pitman, N. J. Holbrook, and J. McAneney, 2007: Evaluation of the AR4 climate models' simulated daily maximum temperature, minimum temperature, and precipitation over Australia using probability density functions. *J. Climate*, **20**, 4356–4376.
- Pleim, J. E., 2007: A combined local and nonlocal closure model for the atmospheric boundary layer. Part II: Application and evaluation in a mesoscale meteorological model. *J. Appl. Meteor. Climatol.*, **46**, 1396–1409.
- Roeckner, E., and Coauthors, 2003: The atmospheric general circulation model ECHAM5. Part I: Model description. MPI Rep. 349, 127 pp.
- Romero, R., C. Ramis, J. Guijarro, and G. Sumner, 1999: Daily rainfall affinity areas in mediterranean Spain. *Int. J. Climatol.*, **19**, 557–578.
- Rosenberg, E. A., P. W. Keys, D. B. Booth, D. Hartley, J. Burkey, A. C. Steinemann, and D. P. Lettenmaier, 2010: Precipitation extremes and the impacts of climate change on stormwater infrastructure in Washington State. *Climatic Change*, **102**, 319–349.
- Rummukainen, M., 2010: State-of-the-art with regional climate models. *Wiley Interdiscip. Rev: Climate Change*, **1**, 82–96.
- Skamarock, W. C., and Coauthors, 2008: A description of the Advanced Research WRF version 3. NCAR Tech. Note NCAR/TN-475+STR, 125 pp. [Available online at http://www.mmm.ucar.edu/wrf/users/docs/arw_v3.pdf.]
- Solomon, S., and Coauthors, 2007: Technical summary. *Climate Change 2007: The Physical Science Basis*, S. Solomon et al., Eds., Cambridge University Press, 19–91.
- Sotillo, M. G., C. Ramis, R. Romero, S. Alonso, and V. Homar, 2003: Role of orography in the spatial distribution of precipitation over the Spanish Mediterranean zone. *Climate Res.*, **23**, 247–261.
- Stensrud, D. J., 2007: *Parameterization Schemes: Keys to Understanding Numerical Weather Prediction Models*. Cambridge University Press, 459 pp.
- Uppala, S. M., and Coauthors, 2005: The ERA-40 Re-Analysis. *Quart. J. Roy. Meteor. Soc.*, **131**, 2961–3012.
- von Storch, H., H. Langenberg, and F. Feser, 2000: A spectral nudging technique for dynamical downscaling purposes. *Mon. Wea. Rev.*, **128**, 3664–3673.
- Waldron, K., J. Paegle, and J. Horel, 1996: Sensitivity of a spectrally filtered and nudged limited-area model to outer model options. *Mon. Wea. Rev.*, **124**, 529–547.
- Walsh, K., and J. McGregor, 1997: An assessment of simulations of climate variability over Australia with a limited area model. *Int. J. Climatol.*, **17**, 201–223.